Geophys. J. R. astr. Soc. (1971) **25**, 447–467.

Electromagnetic Induction in Thin Finite Sheets Having Conductivity Decreasing to Zero at the Edge, with Geomagnetic Applications—II

Attia A. Ashour

(Received 1971 July 13)*

Summary

Electromagnetic induction in a perfectly conducting spherical shell covered by a concentric non-uniformly conducting hemispherical shell by an external magnetic field is considered. The two conductors represent the Earth's conductivity and a large ocean respectively. The integrated conductivity of the outer shell is axisymmetric and reaches a maximum before tending to zero at the edge, hence it is continuous there. The parameters of the problem allow for the consideration of the effects of different periods of variation, different depths of the conducting core and different locations of the edge of the continental shelf.

Spherical harmonics are used and the properties of certain vector functions involving Legendre functions are given. The problem is then reduced to the solution of an infinite system of linear equations.

The effects of a uniform inducing field are considered in the two cases when its direction is either parallel or normal to the axis of symmetry. The results indicate that the components of the observed field are enhanced in sea and land in the vicinity of the coastline. This enhancement is more pronounced if the continental shelf is near the coastline and for the shorter periods of variations. The effect of taking the Earth's conductivity into account is to reduce the enhancement of the field near the coast.

The analysis and the computer program can both be adapted to allow for the estimation of the modification to the external field at any particular station with no conductivity anomaly in the vicinity.

1. Introduction

In a previous paper (1971), which will be referred to hereafter as Paper I, electromagnetic induction in thin sheets of the forms of an infinite strip of uniform width, a circular disk and a hemispherical shell was considered. The conductivity in each case was assumed continuous and zero at the boundary of the sheet. The inducing field considered was uniform and normal to the plane of the sheet in the first two cases and a certain axisymmetric dipole in the third. The effects of periodic time variations of the inducing field, and also of a sudden rise in it were considered. The results were applied to investigate the effects of a large ocean on geomagnetic variations with special consideration of these effects in the vicinity of the coastline. The induced

* Received in original form 1971 March 15

field (and the total field) was found to be continuous and finite at the boundary. The results also showed that the vertical component of the total field is enhanced in the vicinity of the coastline in land and in sea, but it is not reversed as the coastline is traversed. It was also found that the horizontal component is enhanced in sea and reaches its maximum at the edge of the continental shelf, then decreases to an insignificant value at the coastline and in land. It was concluded that the enhancement in the components of the field should be observable for periods of up to 24 hr and within few skin depths from the coastline in the case of periodic variations. In the case of very rapid variations the enhancement should be observable for a time of the order of 1 hr after the change occurs.

The models considered in Paper I, however, did not allow for the conductivity of the Earth. Also the discussion was limited to axisymmetric fields in the cases of the disk and hemispherical shell and to fields which render the problem two-dimensional in the case of the infinite strip. In particular, because the solution for the hemispherical shell was obtained from that for the disk by using a certain inversion process (Ashour 1965), the inducing field considered in this case was an axisymmetric dipole situated at the pole external to the hemisphere.

In the present paper, the work in Paper I is extended to take account of the conductivity of the underlying Earth and to allow the effects of any inducing field to be found. The work is confined to spherical models and a direct method of solution (not depending on the disk) is used. Thus we consider a model of two conductors: a perfectly conducting spherical shell to represent the conductivity of the Earth and a concentric non-uniform hemispherical shell of larger radius to represent the ocean. The conductivity of the outer conductor is axisymmetric and rises to a maximum before dropping to zero at the boundary; it is not however identical with the conductivity distribution considered in Paper I. Three such conductivity distributions are considered in order to investigate the effect of the location of the edge of the continental shelf on the enhancement of the field components.

In the application, the effects due to a uniform inducing field either parallel or normal to the axis of symmetry are considered. Clearly, the effects of any other uniform field can be obtained from the results of these two cases. Only periodic time variations of the inducing field are considered. Aperiodic variations, which pose a different mathematical problem, will be considered in a following paper.

The results are in general agreement with those obtained in Paper I, i.e. the induced field, though finite and continuous at the coastline is enhanced there and in the vicinity and the enhancement is more pronounced for the shorter periods. They show further that the enhancement is very much reduced if the ocean's depth decreases gradually to zero at the coastline, i.e. if the edge of the continental shelf is relativity far from the coastline. The position of the edge of the continental shelf is thus a determinental factor in the coastline effect.

The effect of the conductivity of the Earth is found to be reduction of the componenets of the total field in the vicinity of the coastline and the continental shelf to a ratio ranging between 66 per cent and 75 per cent of their values when only the effect of the ocean is considered. Hence, it would not ' conceal ' the effect of the ocean, specially for the shorter periods of variations.

For periods of up to 24 hr, the effects should be observable in land and sea within few hundreds of kilometres of the coastline, provided that the edge of the continental shelf is itself within about 1000 km from the coastline.

2. The conducting model and the corresponding mathematical problem

2.0. *The model*

Let r, θ, ϕ be spherical polar co-ordinates. We consider a system of two conductors: a perfectly conducting shell $r = b$ (to represent the Earth's conductivity) and a concentric non-uniform hemispherical shell $r = a(> b), 0 \leqslant \theta \leqslant \pi/2$ (to represent the

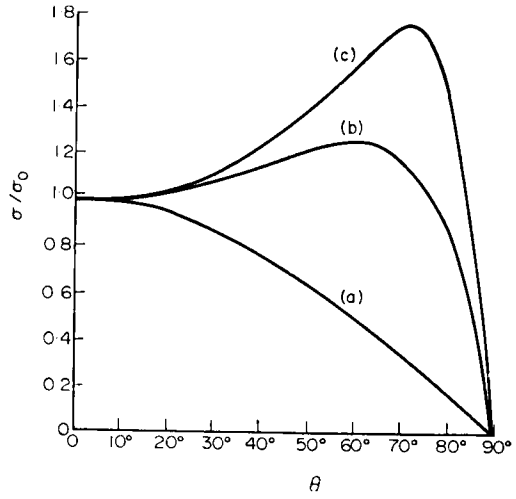

FIG. 1. The distribution of conductivity over the outer shell

$$\sigma = \sigma_0(1+\alpha)\cos\theta/(1+\alpha\cos^2\theta)$$

(*a*) $\alpha = 0$: $\sigma_{max} = \sigma_0$ at $\theta = 0$, $\bar{\sigma}$(average) $= \sigma_0/2$

(*b*) $\alpha = 4$: $\sigma_{max} = 1{\cdot}25\sigma_0$ at $\theta = 60°$, $\bar{\sigma} = \sigma_0$

(*c*) $\alpha = 10$: $\sigma_{max} = 1{\cdot}74\sigma_0$ at $\theta = 72°$, $\bar{\sigma} = 1{\cdot}32\sigma_0$

ocean), we assume the magnetic permeability to be one everywhere and the medium outside the conductors to be non-conducting. The integrated conductivity $\sigma(\theta)$ of the outer conductor is assumed to be given by

$$\sigma(\theta) = \sigma_0(1+\alpha)\cos\theta(1+\alpha\cos^2\theta)^{-1} \tag{1}$$

where σ_0, α are positive finite constants. Thus the integrated conductivity is zero at the boundary of the shell ($\theta = \pi/2$). Fig. 1 shows the variation of σ with θ for the three values of α which will be considered later in the calculations, namely $\alpha = 0$, 4 and 10. For $\alpha = 0$, the conductivity (and hence the depth of the ocean) decreases gradually from a maximum at the centre of the ocean to zero at the coastline. For the non-zero values of α, the conductivity first increases to a maximum *, then decreases to zero at the edge. When $\alpha = 4$, the maximum is $1{\cdot}25\sigma_0$ and occurs at $\theta = 60°$ and when $\alpha = 10$, the maximum is $1.74\sigma_0$ at $\theta = 72°$. The average integrated conductivity $\bar{\sigma}$ is given by

$$\bar{\sigma} = \{\sigma_0(1+\alpha)/2\alpha\}\log(1+\alpha) \tag{2}$$

and is equal to $\sigma_0/2$, $1{\cdot}006\sigma_0$, $1{\cdot}319\sigma_0$ respectively for the three mentioned values of α.

2.1. *The inducing and induced fields*

We shall consider a time varying inducing field of external origin. Hence the magnetic vector potential of both the inducing and induced fields will satisfy the equations

$$\nabla^2\mathbf{A} = 0,\ \operatorname{div}\mathbf{A} = 0 \tag{3}$$

outside the conductors. As explained in Paper I, the solution of equations (3) assumes relatively simple forms when the field is axisymmetric. We shall deal here with both symmetrical and non-symmetrical fields. Hence the general solution of (3) in spherical polar co-ordinates is needed. This can be written as (Smythe 1968):

* The location of the maximum for the model considered in Paper I occurred at $\theta = 83{\cdot}3°$.

$$\mathbf{A} = \text{curl}\,(\mathbf{r}U + \mathbf{r} \wedge \text{grad}\, V) \tag{4}$$

where $\mathbf{r}$ is the position vector and U, V are scalar potential functions. The term involving V does not contribute to the magnetic field $\mathbf{H}\,(= \text{curl}\,\mathbf{A})$ and hence can be ignored without loss of generality. Due to the linearity of the equations governing the induction of currents, we may further assume that the inducing field is arising from one spherical harmonic only. The effects of other harmonics can be obtained by superposition. Hence, for the vector potential $\mathbf{A}^e$ of the inducing field, we take

$$\mathbf{A}^e = \text{curl}\,(\mathbf{r}U^e) \tag{5}$$

where

$$U^e = (a/2)\,H_0(t)(r/a)^N\,P_N^m(u)\cos m\phi, \tag{6}$$

$H_0(t)$ is a time factor, N, m are positive integers, $u = \cos\theta$ and $P_N^m(u)$ is the Legendre associated function of degree N and order m in u. Similarly, the vector potential $\mathbf{A}^i$ of the induced field can be expressed as

$$\mathbf{A}^i = \text{curl}\,(\mathbf{r}U^i) \tag{7}$$

where

$$U^i = aH_0(t)\sum_{n=m}^{\infty} f_n(r)\,P_n^m(u)\cos m\phi, \tag{8}$$

$$\left.\begin{aligned} f_n(r) &= A_n(r/a)^{-n-1} && r \geqslant a \\ &= B_n(r/a)^n + C_n(r/a)^{-n-1} && b \leqslant r \leqslant a \end{aligned}\right\} \tag{9}$$

and A_n, B_n, C_n are time factors to be determined. In (8), harmonics of one order only (m) appear. This is justified by virtue of the boundary condition (21) and the fact that the conductivity is independent of ϕ. The above form for $\mathbf{A}^i$ insures that it is finite everywhere. Using (7) and (8), $\mathbf{A}^i$ can be expressed as

$$\mathbf{A}^i = aH_0(t)\sum_{n=m}^{\infty} \mathbf{W}_n(\theta,\phi) f_n(r) \tag{10}$$

where

$$\mathbf{W}_n(\theta,\phi) = -m\,\text{cosec}\,\theta\,P_n^m(u)\sin m\phi\boldsymbol{\Theta} + \sin\theta P'^m_n(u)\cos m\phi\boldsymbol{\Phi}, \tag{11}$$

$\boldsymbol{\Theta}$, $\boldsymbol{\Phi}$ are unit vectors in the directions of increasing θ, and ϕ respectively. We shall consider the properties of the vector functions $\mathbf{W}_n$ later. The normal and tangential components of the induced field are given by

$$Z^i = \frac{\partial^2}{\partial r^2}(rU^i) = \frac{H_0\,a}{r}\cos m\phi\sum_{n=m}^{\infty} n(n+1) f_n(r)\,P_n^m(u) \tag{12}$$

$$H_\theta{}^i = \frac{1}{r}\frac{\partial^2}{\partial r\partial\theta}(rU^i) = \frac{H_0\,a\sin\theta\cos m\phi}{r}\sum_{n=m}^{\infty} F_n(r)\,P'^m_n(u) \tag{13}$$

$$H_\phi{}^i = \frac{1}{r\sin\theta}\frac{\partial}{\partial r}\left(r\frac{\partial U^i}{\partial\phi}\right) = \frac{mH_0\,a\cos\theta\sin m\phi}{r}\sum_{n=m}^{\infty} F_n(r)\,P_n^m(u) \tag{14}$$

where

$$F_n(r) = -d(rf_n(r))/dr. \tag{15}$$

Since the conductivity of the outer shell is zero at its boundary, the current density will also be zero and continuous there. It has been shown in Paper I, that the induced field is finite and continuous at the boundary. Although the conductivity distributions assumed here and in Paper I are not identical, they have the same features. Hence,

we also expect the induced field here to be continuous and finite at the boundary and there is no danger in the series (12), (13) or (14) being divergent at the boundary as in the case when the conductivity is discontinuous there.

2.2. *Boundary conditions*

In addition to the condition to be satisfied by the inducing and induced fields at the surface of the outer shell, we have two boundary conditions:

(i) The normal component of the induced field is continuous on crossing the surface $r = a$.

(ii) The normal component of the total field vanishes at the perfectly conducting surface $r = b$.

Using (9), (12) and the orthogonal property of the Legendre functions, (i) gives

$$A_n = B_n + C_n. \tag{16}$$

Similarly, using (5), (6), (9) and (12), (ii) yields

$$\left.\begin{aligned} C_n &= -\nu^{2n+1} B_n && n \neq N \\ C_N &= -\nu^{2N+1} (B_N + \tfrac{1}{2}) \end{aligned}\right\} \tag{17}$$

where

$$\nu = b/a. \tag{18}$$

Using (16), (17), we obtain

$$\left.\begin{aligned} A_n &= \mu_n B_n && n \neq N \\ A_N + \tfrac{1}{2} &= \mu_N (B_N + \tfrac{1}{2}) \end{aligned}\right\} \tag{19}$$

where

$$\mu_n = 1 - \nu^{2n+1}. \tag{20}$$

The condition to be satisfied by the vector potentials of the inducing and induced fields at the closed surface of which a thin finite non-uniform sheet is a part has been given in general form in Paper I. In the present case, this condition for the surface $r = a$ becomes

$$\left.\begin{aligned} [\partial \mathbf{A}_s{}^i/\partial r] &= 4\pi\sigma(\theta)\, \partial(\mathbf{A}_s{}^i + \mathbf{A}_s{}^e)/\partial t && r = a,\ 0 \leqslant \theta \leqslant \pi/2 \\ &= 0 && r = a,\ \pi/2 \leqslant \theta \leqslant \pi \end{aligned}\right\} \tag{21}$$

where $[F]$ denotes the change in the function F on crossing the surface $r = a$, and $\mathbf{A}_s$ is the vector tangential component of $\mathbf{A}$ (here $\mathbf{A}_s = \mathbf{A}$ since the vector potentials do not have a normal component).

We note here that it does not suffice to apply (21) to *one tangential component only* (i.e. to $A_\theta{}^i$ only or to $A_\phi{}^i$ only). The application of (21) to $\mathbf{A}_s{}^i$ insures that both components are being considered.

Substituting from (1), (5), (6), (8), (9), (10), (17) and (19) in (21), the latter is reduced to

$$\left.\begin{aligned} &\{(1+\alpha u^2)/(1+\alpha)\} \sum_{n=m}^{\infty} (2n+1)\, B_n \mathbf{W}_n(\theta, \phi) \\ &\qquad = -4\pi\sigma_0\, Du \sum_{n=m}^{\infty} \mu_n B_n{}' \mathbf{W}_n(\theta, \phi) && 0 \leqslant \theta \leqslant \pi/2 \\ &\qquad = 0 && \pi/2 \leqslant \theta \leqslant \pi \end{aligned}\right\} \tag{22}$$

where

$$\left.\begin{aligned} B_n' &= B_n \quad n \neq N \\ B_N' &= B_N + \tfrac{1}{2} \end{aligned}\right\} \tag{23}$$

and D denotes the operator $\partial/\partial t$.

2.3. *The system of linear equations for the coefficients B_n*

Equation (22) can be utilized to obtain an infinite system of linear equations for the unknown coefficients B_n. For this purpose, we first prove the orthognality of the vector functions $\mathbf{W}_n(\theta, \phi)$. If we integrate the scalar product of the functions of orders n and l over the surface Σ of the unit sphere, i.e. with respect to ϕ from $-\pi$ to π, and with respect to u from -1 to 1, we obtain

$$\begin{aligned} \int\int_{\Sigma} \mathbf{W}_n.\mathbf{W}_l\, d\Sigma &= \int_{-\pi}^{\pi} \int_{-1}^{1} \mathbf{W}_n.\mathbf{W}_l\, d\phi\, du \\ &= \frac{2\pi}{2-\delta_m{}^0} \int_{-1}^{1} \{m^2(1-u^2)^{-1} P_l^m P_n^m + (1-u^2) P'^m_n P'^m_l\}\, du \end{aligned} \tag{24}$$

where

$$\left.\begin{aligned} \delta_m{}^0 &= 0 \quad m \neq 0 \\ &= 1 \quad m = 0 \end{aligned}\right\}. \tag{25}$$

Noting that $P_l^m(u)$ satisfies the differential equation

$$\frac{d}{du}\left\{(1-u^2)\frac{dP^m}{du}\right\} + \left\{ l(l+1) - m^2(1-u^2)^{-1}\right\} P_l^m = 0 \tag{26}$$

we obtain

$$\begin{aligned} \int\int_{\Sigma} \mathbf{W}_n.\mathbf{W}_l\, d\Sigma &= \frac{2\pi}{2-\delta_m{}^0}\left\{\int_{-1}^{1} \frac{d}{du}\{(1-u^2) P'^m_l P_n^m\}\, du + l(l+1)\int_{-1}^{1} P_n^m P_l^m\, du\right\} \\ &= 0 \qquad\qquad\qquad\qquad\qquad\qquad\qquad\qquad n \neq l \\ &= \frac{4\pi}{(2-\delta_m{}^0)}\cdot\frac{1}{(2n+1)}\cdot\frac{(n+m)!}{(n-m)!} \qquad n = l \end{aligned} \tag{27}$$

The integration of the product $\mathbf{W}_n.\mathbf{W}_l$ over *half* the surface of the unit sphere given by $-\pi \leqslant \phi < \pi$ and $0 \leqslant \theta \leqslant \pi/2$ will also be needed. If we denote this half surface by Σ', we obtain as before

$$\int\int_{\Sigma'} \mathbf{W}_n.\mathbf{W}_l\, d\Sigma = \frac{2\pi}{2-\delta_m{}^0}\left\{ l(l+1)\int_{0}^{1} P_n^m P_l^m\, du - P_n^m(0)\, P'^m_l(0)\right\}.$$

The integral thus vanishes if $n+l$ is even and $n \neq l$ because in this case the integrand of the integral on the R.H.S. is even and hence the value of the integral is half that with limits -1 and 1, i.e. zero. Also in this case either $P_n^m(0)$ or $P'^m_l(0)$ is zero. If $n = l$, the value of the integral is half the corresponding value in (27). If $n+l$ is odd, we may take without loss of generality $n+m$ to be odd and $l+m$ to be even. In this case, the second term on the R.H.S. vanishes. Hence

$$\left.\begin{aligned}
&= 0 && n+l \text{ even}, \ n \neq l \\
\int_{\Sigma'}\int \mathbf{W}_n.\mathbf{W}_l\, d\Sigma &= \frac{2\pi}{2-\delta_m{}^0}\cdot\frac{1}{2n+1}\cdot\frac{(n+m)!}{(n-m)!} && n = l \\
&= \frac{2\pi l(l+1)}{2-\delta_m{}^0}\, I(n, l; m) && n+m \text{ odd}, \ l+m \text{ even}
\end{aligned}\right\} \quad (28)$$

where (Ashour 1964),

$$I(n, l; m) = \int_0^1 P_n^m\, P_l^m\, du$$

$$= (-1)^{(l-n-1)/2}\,\frac{1.3\ldots(l+m-1)}{2.4\ldots(l-m)}\cdot\frac{1.3\ldots(n+m)}{2.4\ldots(n-m-1)}\cdot\frac{1}{(l-n)(l+n+1)}$$

$$l+m \text{ even}, \ n+m \text{ odd}. \quad (29)$$

We shall need two more integrals I_1 and I_2:

$$I_1 = \int_\Sigma\int u \sin\theta\, P_n^m(u) \cos m\phi\, \boldsymbol{\Phi}.\mathbf{W}_l\, d\Sigma$$

$$= \frac{2\pi}{2-\delta_m{}^0}\int_{-1}^1 u(1-u^2)\, P_n^m\, P'_l{}^m\, du.$$

Using the recurrence relations

$$(2n+1)\, uP_n^m(u) = (n-m+1)\, P_{n+1}{}^m(u)+(n+m)\, P_{n-1}{}^m(u) \quad (30)$$

$$(2l+1)(1-u^2)\, P'_l{}^m(u) = -l(l-m+1)\, P_{l+1}{}^m(u)+(l+1)(l+m)\, P_{l-1}{}^m(u) \quad (31)$$

we obtain after considerable reduction

$$\frac{(2-\delta_m{}^0)}{4\pi} I_1 = \left\{\begin{aligned}
&0 && l \neq n \text{ or } n\pm 2 \\
&\frac{[l(l+1)-3m^2]}{(2l-1)(2l+1)(2l+3)}\cdot\frac{(l+m)!}{(l-m)!} && l = n \\
&\frac{(l+1)}{(2l-3)(2l-1)(2l+1)}\cdot\frac{(l+m)!}{(l-m-2)!} && l = n+2 \\
&\frac{-l}{(2l+1)(2l+3)(2l+5)}\cdot\frac{(l+m+2)!}{(l-m)!} && l = n-2
\end{aligned}\right\} \quad (32)$$

$$I_2 = \int_{\Sigma'}\int \sin\theta\, P_n^m(u) \cos m\phi\, \boldsymbol{\Phi}.\mathbf{W}_l\, d\Sigma$$

$$= \frac{2\pi}{2-\delta_m{}^0}\int_0^1 (1-u^2)\, P_n^m\, P'_l{}^m\, du \ .$$

Using (29) and (31) we obtain

$$\frac{(2-\delta_m{}^0)}{2\pi} I_2 = \left\{ \begin{array}{ll} 0 & n+l \text{ odd},\ n \neq l \pm 1 \\ \dfrac{(l+1)}{(2l-1)} \cdot \dfrac{(l+m)!}{(l-m-1)!} & n = l-1 \\ \dfrac{-l}{(2l+3)} \cdot \dfrac{(l+m+1)!}{(l-m)!} & n = l+1 \\ (2l+1)^{-1} \{(l+1)(l+m)\, I(n, l-1; m) - l(l+1-m)\, I(n, l+1; m)\} & n+l \text{ even} \end{array} \right\} \quad (33)$$

Finally using the recurrence relation (30) and (11), we obtain

$$u\mathbf{W}_n(\theta, \phi) = (2n+1)^{-1} \{(n-m+1)\, \mathbf{W}_{n+1} + (n+m)\, \mathbf{W}_{n-1}\} - \sin\theta \cos m\phi P_n^m(u)\, \boldsymbol{\Phi} \quad (34)$$

and

$$(1+\alpha u^2)\, \mathbf{W}_n(\theta, \phi) = \frac{(n+m-1)(n-m+2)\alpha}{(2n+1)(2n+3)} \mathbf{W}_{n+2} + \left\{1 + \frac{(2n^2+2n-2m^2-1)\,\alpha}{(2n-1)(2n+3)}\right\} \mathbf{W}_n + \frac{(n+m-1)(n+m)\alpha}{(2n-1)(2n+1)} \mathbf{W}_{n-2} - 2\alpha u \sin\theta \cos m\phi\, P_n^m(u)\, \boldsymbol{\Phi}. \quad (35)$$

We now multiply both sides of (22)scalarly by $\mathbf{W}_l(\theta, \phi)$ and integrate over the whole surface Σ of the unit sphere. The integration of the R.H.S. will clearly be over half the surface of the sphere only, i.e. over Σ', since this side vanishes for $\pi/2 \leqslant \theta \leqslant \pi$. Eliminating the common factor $4\pi/(2-\delta_m{}^0)$ from both sides, we obtain for the L.H.S. (which we shall denote by L) using (35), (27) and (32)

$$L = \beta_l B_{l-2} + \gamma_l B_l + \varepsilon_l B_{l+2} \quad (36)$$

where

$$\left. \begin{aligned} \beta_l &= \frac{(l-2)(l+1)}{(2l-1)(2l+1)} \cdot \frac{(l+m)!}{(l-m-2)!} \cdot \frac{\alpha}{(\alpha+1)} \\ \gamma_l &= \left\{ \frac{l(l+1)}{\alpha+1} + \frac{\{2l^2(l+1)^2 - l(l+1)(2m^2+3) + 6m^2\}\,\alpha}{(2l-1)(2l+3)(\alpha+1)} \right\} \frac{(l+m)!}{(l-m)!} \\ \varepsilon_l &= \frac{l(l+3)}{(2l+1)(2l+3)} \cdot \frac{(l+m+2)!}{(l-m)!} \cdot \frac{\alpha}{(\alpha+1)}. \end{aligned} \right\} \quad (37)$$

For the R.H.S. (which we shall denote by R), using (34), (28), (29) and (33), we obtain after considerable reduction

$$R = -\lambda \left\{ S_{l-1,\,l} B'_{l-1} + S_{l+1,\,l} B'_{l+1} + \sum_{n=m}^{\infty *} S_{n,\,l} B_n' \right\} \frac{(l+m)!}{(l-m)!} \quad (38)$$

where Σ^* indicates that the summation is for $n+l$ even and

$$\lambda = 2\pi a \sigma_0\, D \quad (39)$$

$$\left.\begin{aligned} S_{l-1,\,l} &= \frac{(l-1)(l+1)(l-m)}{(2l-1)(2l+1)}\,\mu_{l-1} \\ S_{l+1,\,l} &= \frac{l(l+2)(l+m+1)}{(2l+1)(2l+3)}\,\mu_{l+1} \end{aligned}\right\} \tag{40}$$

$$(-1)^{(n-l-2)/2}\,S_{n,\,l} = \frac{1.3\ldots(l-m-1)}{2.4\ldots(l+m)} \times \frac{1.3\ldots(n+m-1)}{2.4\ldots(n-m)} \times \frac{\{2(n^2+n)(l^2+l)-m^2(n^2+n+l^2+l-2)\}}{\{(n-l)^2-1\}\{(n+l+1)^2-1\}}\,\mu_n \tag{41a}$$

$n+m$ even, $l+m$ even

$$(-1)^{(n-l-2)/2}\,S_{n,\,l} = \frac{1.3\ldots(l-m)}{2.4\ldots(l+m-1)} \times \frac{1.3\ldots(n+m)}{2.4\ldots(n-m-1)} \times \frac{(n^2+n+l^2+l-2)}{\{(n-l)^2-1\}\{(n+l+1)^2-1\}}\,\mu_n \tag{41b}$$

$n+m$ odd, $l+m$ odd.

The required system of linear equation is given by

$$\mathrm{L} = R,\ l = m, m+1, \ldots\ \infty \tag{42}$$

When $\alpha = 0$, this system reduces to

$$l(l+1)\frac{(l+m)!}{(l-m)!}\,B_l = -\lambda\left\{S_{l-1,\,l}\,B'_{l-1} + S_{l+1,\,l}\,B'_{l+1} + \sum_{n=m}^{\infty *} S_{n,\,l}\,B_n'\right\} \tag{43}$$

2.4 *The uniform inducing field*

If we take $N = 1$, $m = 0$ in (6), we obtain

$$\mathbf{A}^e = \tfrac{1}{2}H_0(t)\,r\sin\theta\,\boldsymbol{\Phi} \tag{44}$$

which is the vector potential of a uniform field of intensity $H_0(t)$ parallel to the axis of symmetry. In this case (as in Paper I) there is no dependence on ϕ. The components of the *total* field at $r = a$ are given by

$$Z(a,\theta) = H_0 \sum_{n=1}^{\infty} n(n+1)\,\mu_n B_n'\,P_n(u) \tag{45}$$

$$H_+(a,\theta) = H_0 \sum_{n=1}^{\infty} n\mu_n B_n'\,P_n^{\,1}(u) - (3H_0/2)\,P_1^{\,1}(u) \tag{46}$$

where the + subscript indicates the value just outside $r = a$, and the B_n satisfy (23) and the system of equations (42) with $N = 1$, $m = 0$.

Similarly, if we take $N = m = 1$ in (6), we obtain the vector potential of a uniform inducing field of intensity $H_0(t)$ perpendicular to the axis of symmetry and parallel to the plane $\phi = 0$. The components of the total field are given in this case by

$$Z(a,\theta,\phi) = H_0 \cos\phi \sum_{n=1}^{\infty} n(n+1)\,\mu_n B_n'\, P_n^1(u) \tag{47}$$

$$H_{\theta+}(a,\theta,\phi) = H_0 \cos\phi \sin\theta \left\{ \sum_{n=1}^{\infty} n\mu_n B_n'\, P'^1_n - \tfrac{3}{2} P'^1_1(u) \right\} \tag{48}$$

$$H_{\phi+}(a,\theta,\phi) = H_0 \sin\phi \operatorname{cosec}\theta \left\{ \sum_{n=1}^{\infty} n\mu_n B_n'\, P_n^1(u) - \tfrac{3}{2} P_1^1(u) \right\} \tag{49}$$

where the B_n satisfy (23) and the system of equations (42) with $N = m = 1$. In the applications, we shall consider the effects of a uniform inducing field either parallel or normal to the axis of symmetry. The effects of a uniform field in any other direction can clearly be obtained from the results for these two cases.

3. Method of solution of the infinite system of equations

When the inducing field varies periodically with the time, we may, in the steady state, take

$$H_0(t) = \mathrm{Re}\,(H_0 \exp(i\omega t)], \tag{50}$$

where $2\pi/\omega$ is the period of variations, and consider only real parts of the expressions. In this case, the operator D may be replaced by $i\omega$ and we have

$$\lambda = 2\pi a \sigma_0\, \omega i. \tag{51}$$

A method of successive approximations to the solution of the system of equations (42) is adopted*. The rth approximation corresponds to ignoring B_n' for $n > r$ and considering the first r equations only. By taking† $r = 1, 2, \ldots$, we obtain a series of approximations for the coefficients B_n'. These in turn can be substituted in the series giving the components of the field and the values of these components from successive steps are compared. The process of approximation is stopped only when the desired accuracy for the field components is reached.

4. Numerical results and applications

4.0 *Numerical values*

In the geomagnetic application, we consider an ocean covering half the Earth. Hence we take $a = 6{\cdot}5 \times 10^8$ cm.

For ν, we take three different values: $\nu = 0$, 0·8 and 0·875. The first corresponds to ignoring the conductivity of the Earth. We consider three periods of the inducing field: 24 hr, 12 hr and 1 hr. We also take

$$\sigma_0 = 4 \times 10^{-11} \times 4 \times 10^5 = 1{\cdot}6 \times 10^{-5} \text{ e.m.u. c.m.}$$

and consider three values for the constant α, namely 0, 4 and 10 respectively. Noting that the conductivity of sea water is 4×10^{-11} e.m.u., (2) gives to the values 2 km, 4·024 km and 5·276 km respectively for the average depth of the ocean corresponding to the above three values of α. The assumed values of a and σ_0 give $\lambda = 4{\cdot}738i$, $9{\cdot}475i$ and $113{\cdot}700i$ corresponding to 24-hr, 12-hr and 1-hr periods respectively.

* See for instance, Chapter 2 on infinite systems of linear equations in 'Approximate Methods of Higher Analysis' by Kantorovich & Krylov (1964).

† It is assumed that $m = 0$ or 1 corresponding to a uniform inducing field.

4.1 *Results*

The process of approximation as explained in Section 3 was programmed such that it is stopped only when the actual series giving the components of the induced field differed in the last two steps by less than 10^{-4} in relative magnitude. For 24- and 12-hr period, the required accuracy was obatined from 40 steps. For 1-hr period, it was necessary to carry the process of approximation 90 steps in order to reach the required accuracy. Hence the present method is most suitable for S_q variations but not for the more rapid variations of periods less than 1 hr. For such variations, a good approximation may be obtained by assuming that the outer conductor is also perfectly conducting. This is indicated by the results of Doss & Ashour (1971), of Paper I, and also of the present work.

The amplitudes and phase angles of the components of the total field are calculated at the surface $r = a$, of which the outer conductor is a part, for the two cases when the uniform inducing field is either parallel or normal to the axis of symmetry.

Results for axisymmetric uniform inducing field. For the sake of comparison, the vertical and horizontal components of the total field when only the inner conductor is present (which corresponds to ignoring the effect of the ocean) are calculated at the surface of the outer conductor $r = a$. If we denote these two components by $\bar{Z}$ and $\bar{H}$ respectively then, since the inner conductor is assumed to be perfectly conducting, elementary theory gives

$$\left.\begin{aligned} \bar{Z}(a,\theta) &= H_0(t)(1-\nu^3)\cos\theta \\ \bar{H}(a,\theta) &= H_0(t)(1+\tfrac{1}{2}\nu^3)\sin\theta \end{aligned}\right\}. \tag{52}$$

Clearly, when $\nu = 0$, (52) gives the components Z^e and H^e of the inducing field at $r = a$. Figs 2 and 3 illustrate the variation of $|\bar{Z}/H_0|$ and $|\bar{H}/H_0|$ with θ.

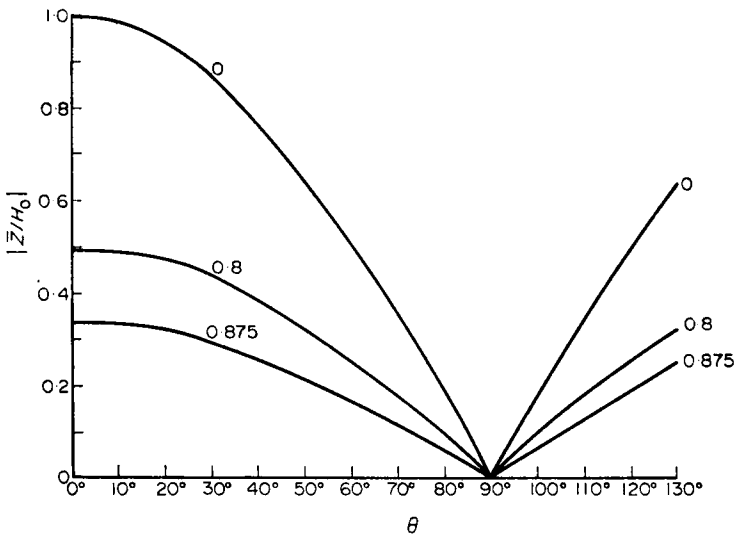

FIG. 2. The vertical component $\bar{Z} = H_0(1-\nu^3)\cos\theta$ of the total field at $r = a$ when a perfect conductor $r = b\ (= \nu a)$ is influenced by a uniform field $H_0(t)$ parallel to the axis $\theta = 0$. The number assigned to each graph indicates the value of ν.

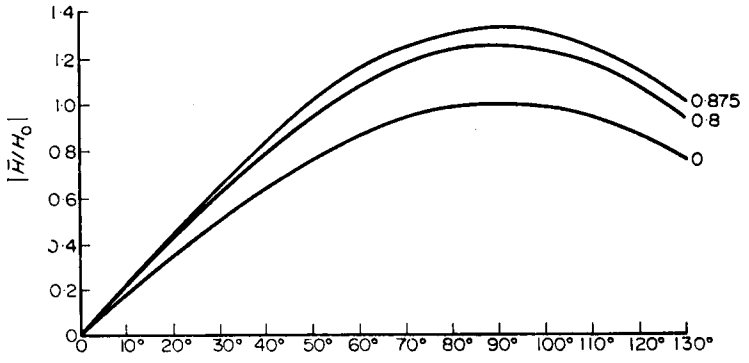

FIG. 3. The horizontal component $\bar{H} = H_0(t)(1 + (\nu^3/2)) \sin\theta$ of the total field at $r = a$ when a perfect conductor $r = b$ $(= \nu a)$ is influenced by a uniform field $H_0(t)$ parallel to the axis $\theta = 0$. The number assigned to each graph indicates the value of ν.

Figs 4 and 5 show $|Z/H_0|$ and $|H/H_0|$ respectively. In each of these two figures, diagrams in a horizontal row (a, b, c; d, e, f; g, h and i) correspond to the same value of α while those in a vertical column correspond to the same value of λ (i.e. to the same period).

It is clear from Fig. 4(a) and (b), that for $\alpha = 0$ (the case of an ocean of gradually decreasing depth) and period of 24 and 12 hr there is no appreciable enhancement of the amplitude of the vertical component in the vicinity of the coast. However, for $\alpha = 0$ and period 1 hr (Fig. 4(c)), the amplitude of the vertical component reaches a maximum in sea just off the coast and is still enhanced in the vicinity of the coast in sea and land. When $\alpha = 4$ (Fig. 4(d), (e) and (f)) we notice a marked difference; the amplitude is enhanced near the coast in sea and land for all three periods considered, the enhancement being more for the shorter periods and less* for the non-zero values of ν. Also the location in sea at which the maximum of the amplitudes occurs gets nearer to the coast as the period of variation gets shorter. The same effects on a larger scale are noticed for $\alpha = 10$ (Fig. 4(g)–(i)).

Comparing the diagrams of Fig. 4 with the graphs of Fig. 2 corresponding to the same value of ν, we see that in the vicinity of the coast, the amplitude of the total vertical component can be several times greater than that of the corresponding component when only the inner conductor is considered.

Comparison of Figs 5(a), (b) with Fig. 4 show that for $\alpha = 0$ and periods of 24 or 12, there is almost no coastline effect on the amplitude of the horizontal component of the total field. For 1-hr period (Fig. 5(c)), the amplitude is enhanced in sea just off the coast, then falls at the coastline and in land to its corresponding values when the effect of the ocean is ignored (Fig. 3). For $\alpha = 4$, we see from comparing Figs 5(d), 5(e) and 5(f) with Fig. 3, that the amplitude of the horizontal component rises in sea to a maximum which ranges between 1.3 and 2 times the corresponding value when only the inner conductor is considered. As for the vertical component, the value of the maximum of the amplitude of the horizontal component is larger for shorter periods, smaller v and larger α. At the coastline itself and in land, there is almost no effect due to the ocean. The graphs for $\alpha = 10$ (Figs 5(g)–(i)) are very similar to the corresponding ones for $\alpha = 4$, except that the location of the maximum in sea is nearer to the coast as might be expected. The effect of taking the Earth's conductivity into account is less for the horizontal component than for the vertical. The change in phase for the

* The amplitude for $\nu = 0{\cdot}8$ and $0{\cdot}875$ is approximately 70 and 55 per cent respectively from its value for $\nu = 0$ (no core).

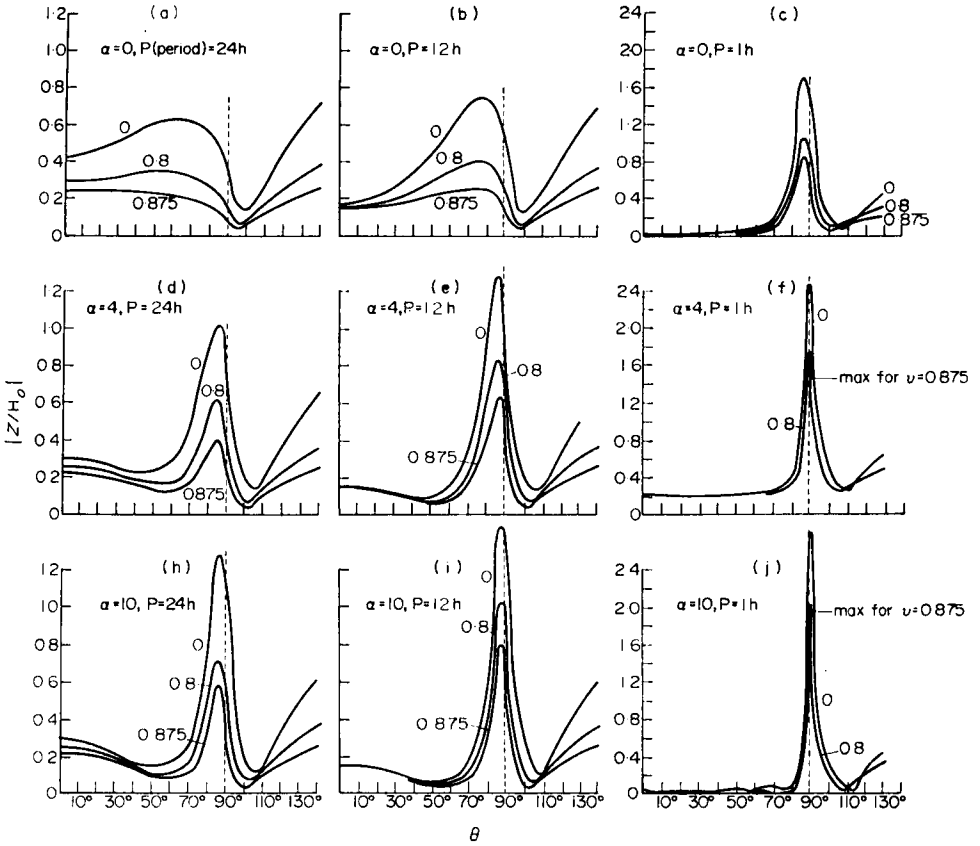

FIG. 4. The amplitude of the vertical component Z of the total field at $r = a$ when the two conductors are present. The inducing field $H_0(t)$ is periodic, uniform and axisymmetric. The period of the field and the value assumed for α are indicated for each diagram. The number assigned to each graph indicates the value of ν for this particular graph. Only the maxima for $\nu = 0{\cdot}875$ are indicates in f and i since the graphs for $\nu = 0{\cdot}8$ and $\nu = 0{\cdot}875$ are almost coincident elsewhere. Note the different vertical scale for c, f and i.

vertical component of the total field near the coastline is gradual and does not correspond to a reversal in this component. The change in phase of the total horizontal component is not important. Fig. 6 illustrated the change in phase of the two components for the particular case: $\alpha = 4$- and 24-hour period.

The angle χ at which the total field is inclined to the vertical ($= \tan^{-1} H/Z$) *was also calculated for the four epochs $t_1 = 0$ (or π/ω), $t_2 = \pi/4\omega$ (or $5\pi/4\omega$), $t_3 = \pi/2\omega$ (or $3\pi/2\omega$) and $t_4 = 3\pi/4\omega$ (or $7\pi/4\omega$). The results obtained for t_1 and t_3 are very similar; also those for t_2 and t_4. Fig. 7 illustrates the change in χ at $t = t_1$ and $t = t_2$. The value of α and the period are indicated on each diagram and those of ν on the corresponding graphs. It will be seen from the figure that at $t = t_1$, no appreciable change occurs in the direction of the total field as the coastline is crossed from sea to land. On the other hand, at $t = t_2$, the direction is turned at the coast into an angle amounting in some cases to 180°, i.e. to a reversal of the direction of the field.

* Here H and Z are the real parts as obtained from the calculations. Results for 24- and 12-hr periods are very close. The same is true for $\alpha = 4$ and $\alpha = 10$ and for $\nu = 0{\cdot}8$ and $\nu = 0{\cdot}875$. Hence we only illustrate the results for 24-hr and 1-hr periods, for $\alpha = 0$ and $\alpha = 10$ and for $\nu = 0$ and $\nu = 0{\cdot}875$.

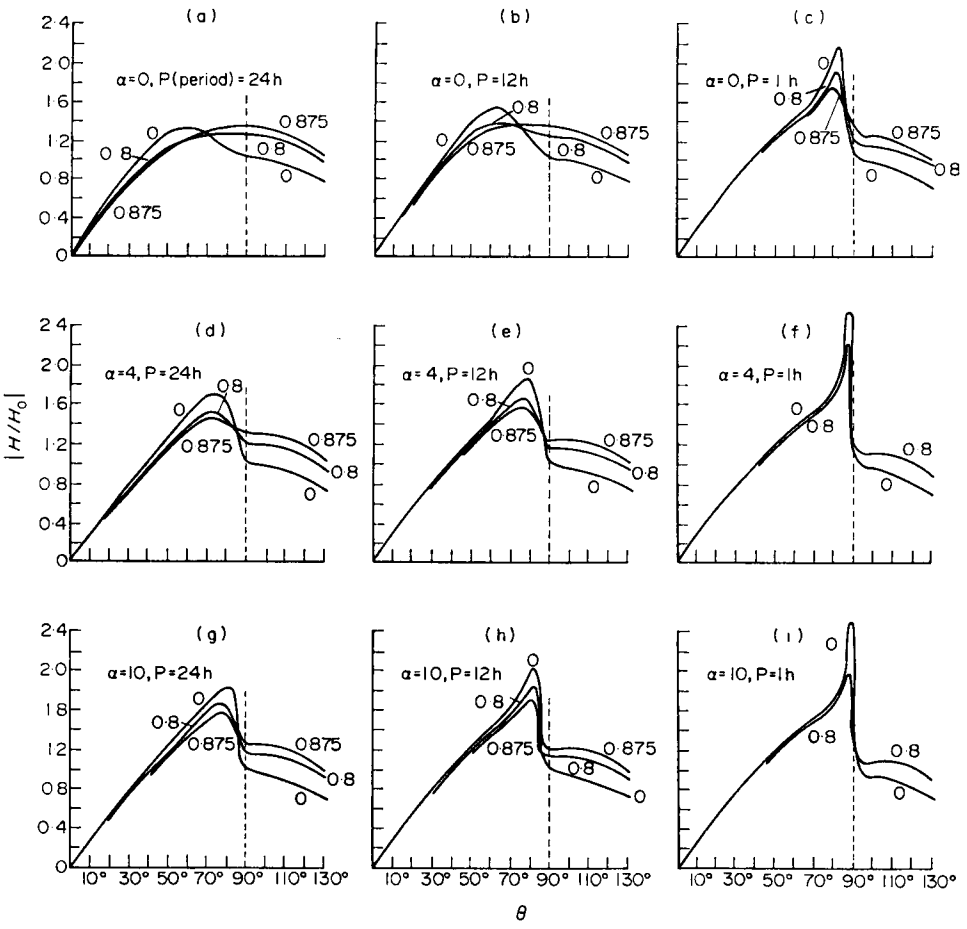

FIG. 5. The amplitude of the horizontal component of the total field at $r = a$. The conductors and the inducing field are as for Fig. 4.

Results for uniform inducing field normal to the axis of symmetry. The field in this case will have two horizontal components in the directions of increasing θ and ϕ respectively. As in the case of the axisymmetric inducing field, we give for comparison, the components of the total field at $r = a$ for the case when only the inner conductor is present. These are

$$\left.\begin{aligned} \bar{Z}(a,\theta,\phi) &= H_0(t)(1-\nu^3)\sin\theta\cos\phi \\ \bar{H}_\theta(a,\theta,\phi) &= H_0(t)(1+(\nu^3/2)]\cos\theta\cos\phi \\ \bar{H}_\phi(a,\theta,\phi) &= -H_0(t)([1+(\nu^3/2)]\sin\phi \end{aligned}\right\} \tag{53}$$

Figs 8 and 9 show $|\bar{Z}/H_0\cos\phi|$ and $|\bar{H}/H_0\cos\phi|$ respectively. The values of $|\bar{H}_\phi/\sin\phi|$ are obvious and there is no need to illustrate them.

The amplitudes and phase angles of the components of the total field are calculated at $r = a$ when both conductors are present. Figs 10, 11 and 12 show $|Z/H_0\cos\phi|$, $|H_\theta/H_0\cos\phi|$ and $|H_\phi/H_0\sin\phi|$ respectively. The arrangement of the diagrams is the same as for the figures in the axisymmetric case (Figs 4 and 5).

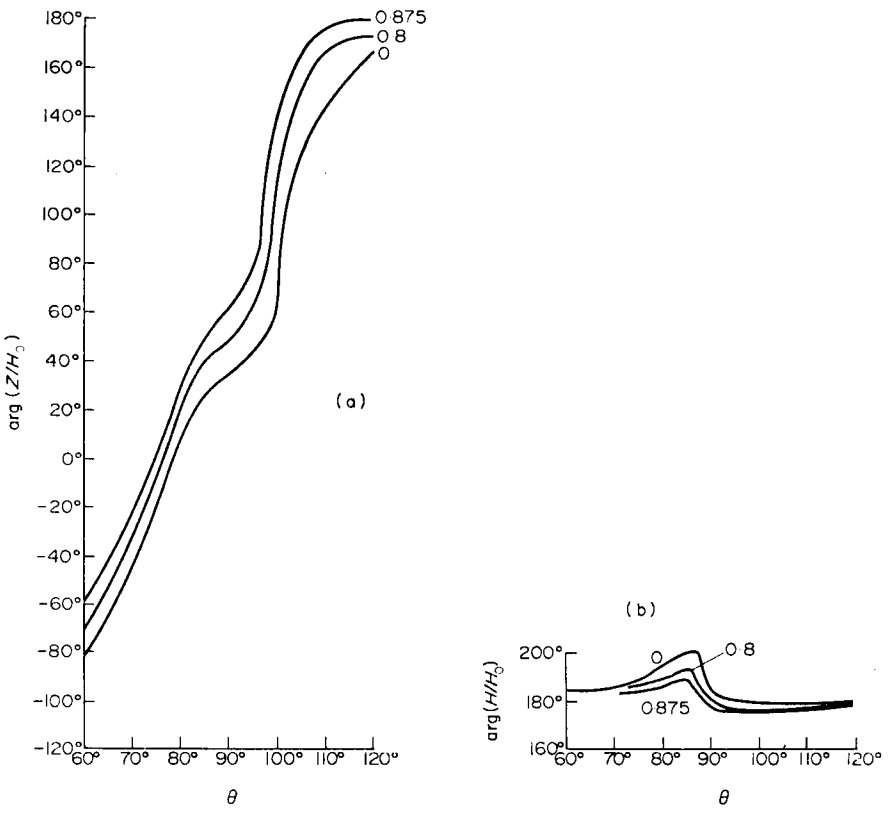

FIG. 6. The change in phase of the components of the total field in the vicinity of the coastline. The conductors and inducing field are as for Fig. 4. The period of variation is 24 hr and $\alpha = 4$. (a) $\arg(Z/H_0(t))$ (b) $\arg(H/H_0(t))$.

The results are similar to those of the axisymmetric inducing field. For $\alpha = 0$ and 24- or 12-hr period (Fig. 10(a) and (b)), there is no significant ocean effect on the total vertical component near the coast; its value there is almost equal to that of the vertical component when only the inner conductor is considered (Fig. 8). For $\alpha = 0$ and one hour period, and $\alpha = 4$- and 24-hr period (Fig. 10(c) and (d)), the amplitude rises to its maximum in sea near the coast more sharply but still does not exceed the corresponding value when only the inner conductor is considered. For $\alpha = 4$ and periods of 12 hr and 1 hr (Fig. 10(e) and (f)), the maximum of the amplitude is larger than the corresponding value when the ocean is ignored and at the coastline itself the amplitude is enhanced compared with the values it assumes in the adjoining land. This effect is more pronounced for the shorter period of one hour. The effect is again further pronounced for $\alpha = 10$. In this case ($\alpha = 10$), as for the axisymmetric case, the maximum of the amplitude occurs almost at the coastline itself.

Comparison of Figs 9 and 11 show that for $\alpha = 0$ there is almost no effect on the amplitude of H near the coast except for the shorter period of 1 hr when the amplitude rises to a maximum near the coast in *sea and in land* (the enhancement in H in the axisymmetric case occurs near the coast in sea only). The effect is again more pronounced for the shorter periods and the larger value of α ($\alpha = 10$).

Fig. 12 shows the amplitude of the other horizontal component in the plane $\phi = \pi/2$. For $v = 0$ (no Earth), the amplitude is greater at the coastline than its constant value when only the Earth is considered. The increase ranges between 20 and

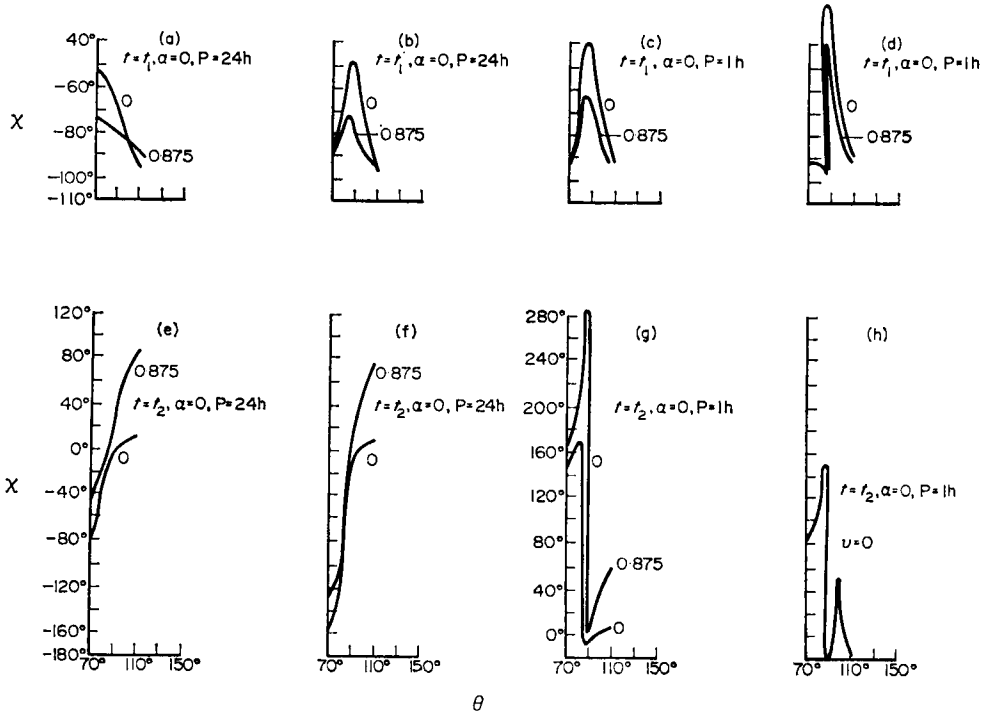

FIG. 7. The angle χ ($= \tan^{-1} H/Z$) at which the direction of the total field (at $r = a$) is inclined to the vertical. The inducing field and the conductors are as for FIG. 4. The values of ν (0 or 0·875), of t ($t_1 = 0$, $t_2 = \frac{1}{4}$ period), of α (0 or 10) and the period of variations are indicated for each diagram. Note the different vertical scale for $t = t_2$. The graph for $\nu = 0{\cdot}875$ is not produced in the last diagram because it almost coincides with that for $\nu = 0$.

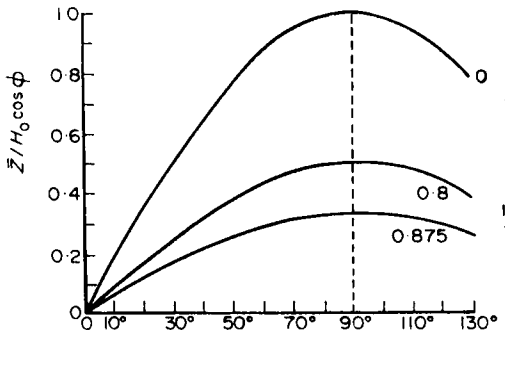

FIG. 8

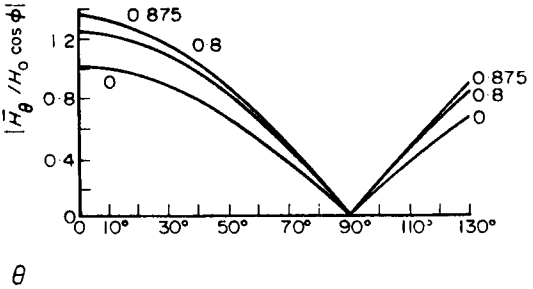

FIG. 9

FIG. 8. The vertical component $\bar{Z} = H_0(t)(1-\nu^3)\sin\theta\cos\phi$ of the total field at $r = a$ when a perfect conductor $r = \nu a$ is influenced by a uniform field $H_0(t)$ normal to the axis of symmetry. The number assigned to each graph indicates the value of ν.

FIG. 9. The component $\bar{H}_\theta = H_0(t)(1+(\nu^3/2))\cos\theta\cos\phi$ of the total field at $r = a$, when a perfect conductor $r = \nu a$ is influenced by a uniform field $H_0(t)$ normal to the axis of symmetry. The number assigned to each graph indicates the value of ν.

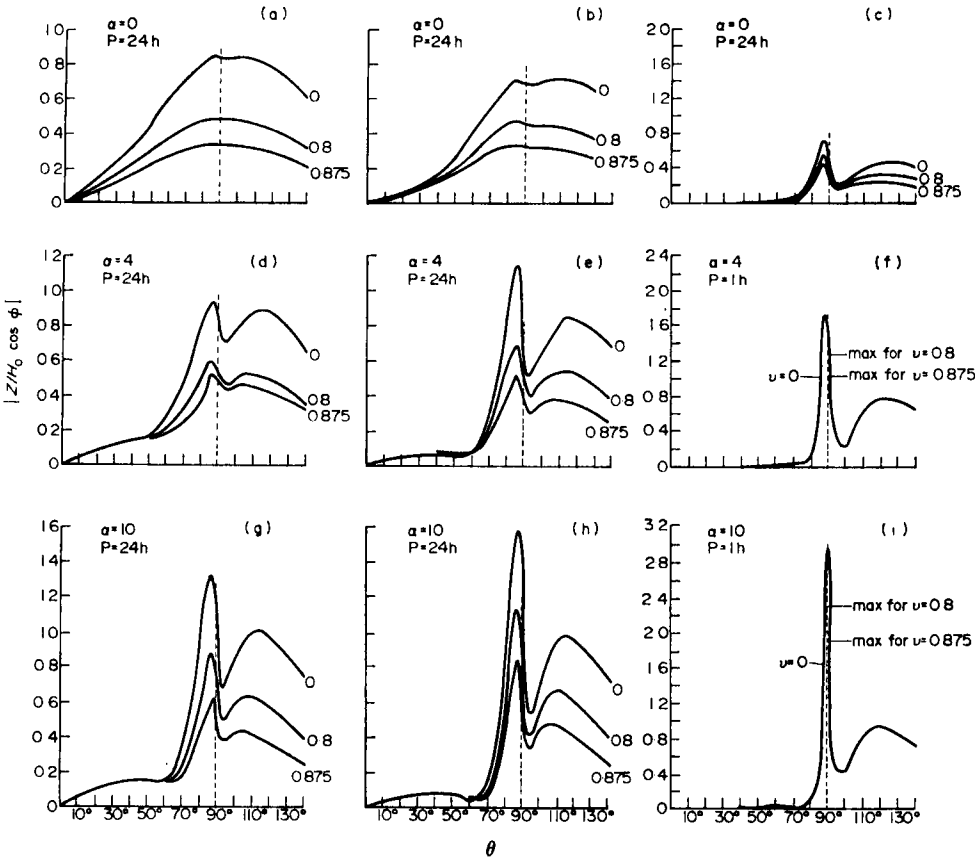

FIG. 10. The amplitude of the vertical component Z of the total field at $r = a$ when the two conductors are present and the inducing field $H_0(t)$ is uniform, periodic and normal to the axis of symmetry. The period of the field and the value of α are indicated on each diagram. The number assigned on each graph indicates the value of ν for this particular graph. Only the maxima for $\nu = 0{\cdot}8$ and $\nu = 0{\cdot}875$ are indicated in figures f and i since otherwise the graphs for $\nu = 0{\cdot}8$ and $0{\cdot}875$ are almost coincident with that for $\nu = 0$. Note the different vertical scale for c, f and i.

60 per cent (from the later value) being larger if α is large and the period is short. However, for $\nu = 0{\cdot}8$ or $0{\cdot}875$, this effect almost disappears.

As for the axisymmetric case, the change in phase for the components of the total field is gradual on crossing the coastline and does not amount to a reversal in any of the components. Fig. 13 illustrates the phase angles of the three components for $\alpha = 4$- and 24-hr period. The graphs for $\alpha = 10$ and the shorter periods are similar to those produced in Fig. 13. The inclination $\chi(= \tan^{-1}\{(H_\theta^2 + H_\phi^2)^{\frac{1}{2}}/Z\}$ of the direction of the total field to the vertical is also calculated for the four epochs $t_1 = 0$, $t_2 = \pi/4\omega$, $t_3 = \pi/2\omega$ and $t_4 = 3\pi/4\omega$ as in the axisymmetric case and also for $\phi = 0$ and $\phi = \pi/4$. The results for $\phi = \pi/4$ indicate little change in the direction of the field near the coastline. Also, when $\phi = 0$ and $\alpha = 0$ the results (for all considered values of ν, the period and t) indicate that the rotation of the direction of the field near the coastline is gradual. However, for $\phi = 0$ and $\alpha \neq 0$, the results obtained show that for periods of 12 or 24 hr, the change in the direction of the field near the coastline is more pronounced for all values of t. For the period of 1 hr, the direction

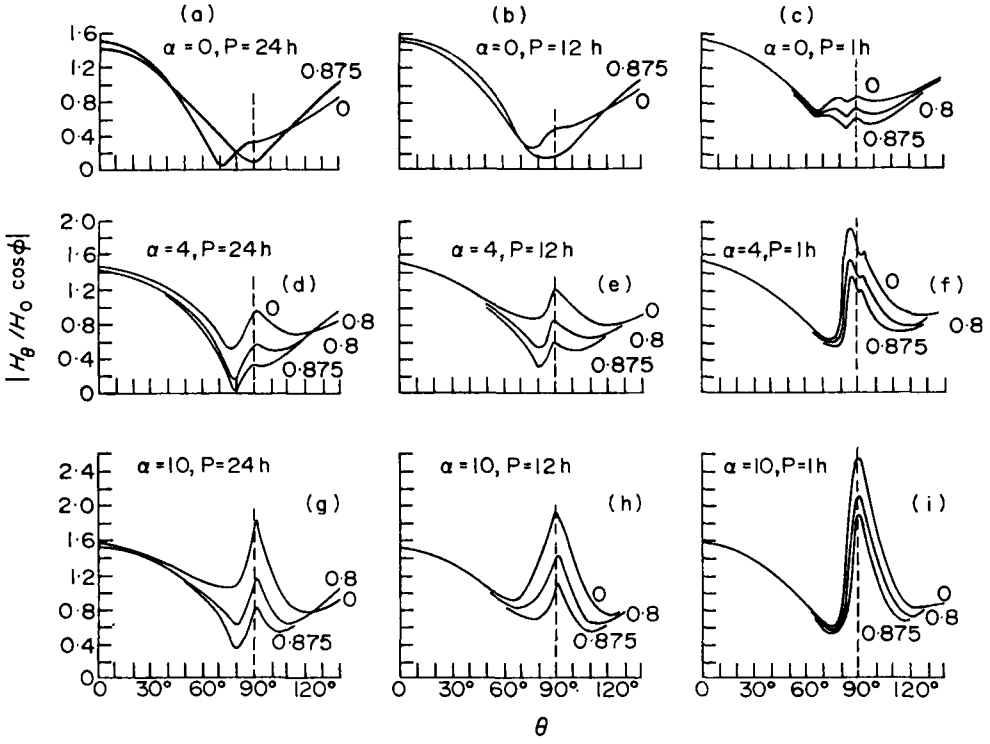

FIG. 11. The amplitude of the horizontal component H_θ of the total field at $r = a$. The conductors and inducing field are as for Fig. 10. In *a* and *b* the graph for $\nu = 0{\cdot}8$ is not produced because it is almost coincident with that for $\nu = 0{\cdot}875$.

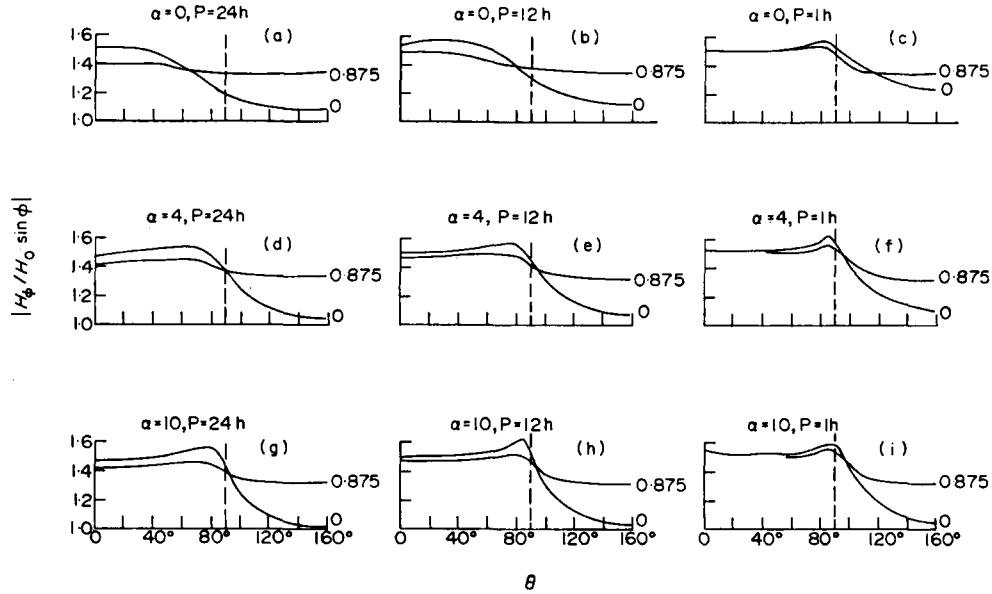

FIG. 12. The amplitude of the horizontal component H_ϕ of the total field at $r = a$. The conductors and inducing field are as for Fig. 10.

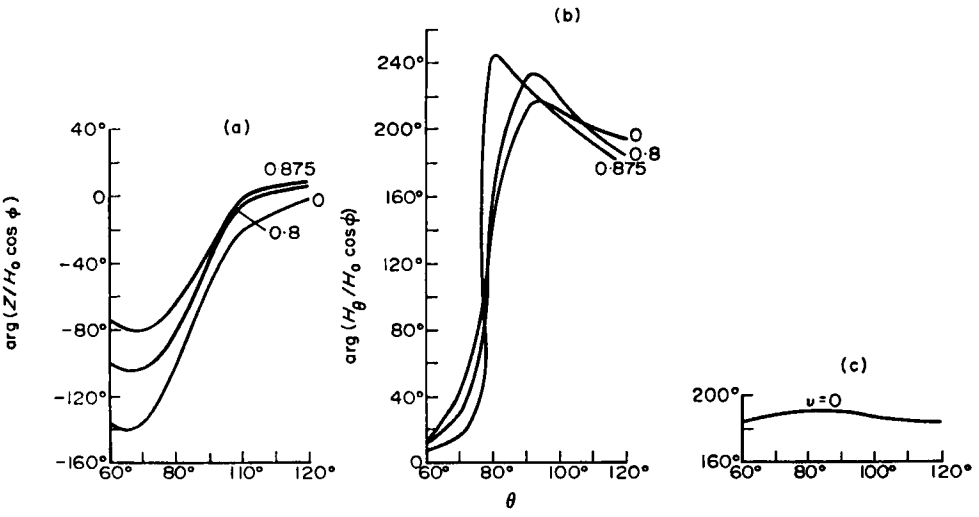

FIG. 13. The change in phase of the components of the total field in the vicinity of the coastline. The conductors and inducing field are the same as for Fig. 10. The period of variations is 24 hr and $\alpha = 4$.
(a) arg $(Z/H_0 \cos\phi)$, (b) arg $(H_\theta/H_0 \cos\phi)$, (c) arg $(H_\phi/H_0 \sin\phi)$. Only the graph for $\nu = 0$ is illustrated, since for the other two values of ν the graph almost coincides with that for $\nu = 0$.

of the field is turned between $\theta = 85°$ and $\theta = 95°$ through an angle of nearly 180° for $t = t_1$, t_3 and t_4. For $t = t_2$, there is a considerable rotation in the direction of the total field on crossing the coastline, but the change does not amount to a complete reversal as for the other values of t.

Fig. 14 shows χ for $\phi = 0$ and $\pi/4$ and $t = t_1$ and t_2. Only results for periods of 24 hr and 1 hr and for $\nu = 0$ and 0·875 are produced.

Conclusions

The present theoretical work is not meant to represent the ocean's effect on geomagnetic variations at any particular station. What is aimed at is to give certain guiding principles to help obtain the primary geomagnetic variation from the observed surface field at any particular station. This process will differ from one station to another depending on the local conditions of the coastline and the continental shelf. The results of the present work and also of Paper I, suggest the following conclusions:

(i) The position of the edge of the continental shelf is a very important factor in the shielding of geomagnetic variations of external origin by a large ocean. If the decrease in depth is gradual from the ocean's centre and does not begin to occur sufficiently near the coastline (as illustrated here by the extreme case $\alpha = 0$), there is almost no enhancement in the observed total field in sea or land for periods of the order of a few hours or more. For periods of 1 hr or less, the field components begin to be enhanced near the coastline.

As the location of the position where the depth begins to decrease gets nearer to the coastline, the components of the total field are enhanced in the vicinity of the coastline for variations of periods up to 24 hr. Even if this location is at a distance of order $a/2$ from the coast of a hemispherical ocean of radius a (the case $\alpha = 4$), the effect will still be manifested at the coastline and in its vicinity.

(ii) In the latter case, which is the more common, and for a uniform inducing field of periodic variations, the amplitude of the vertical component of the total field

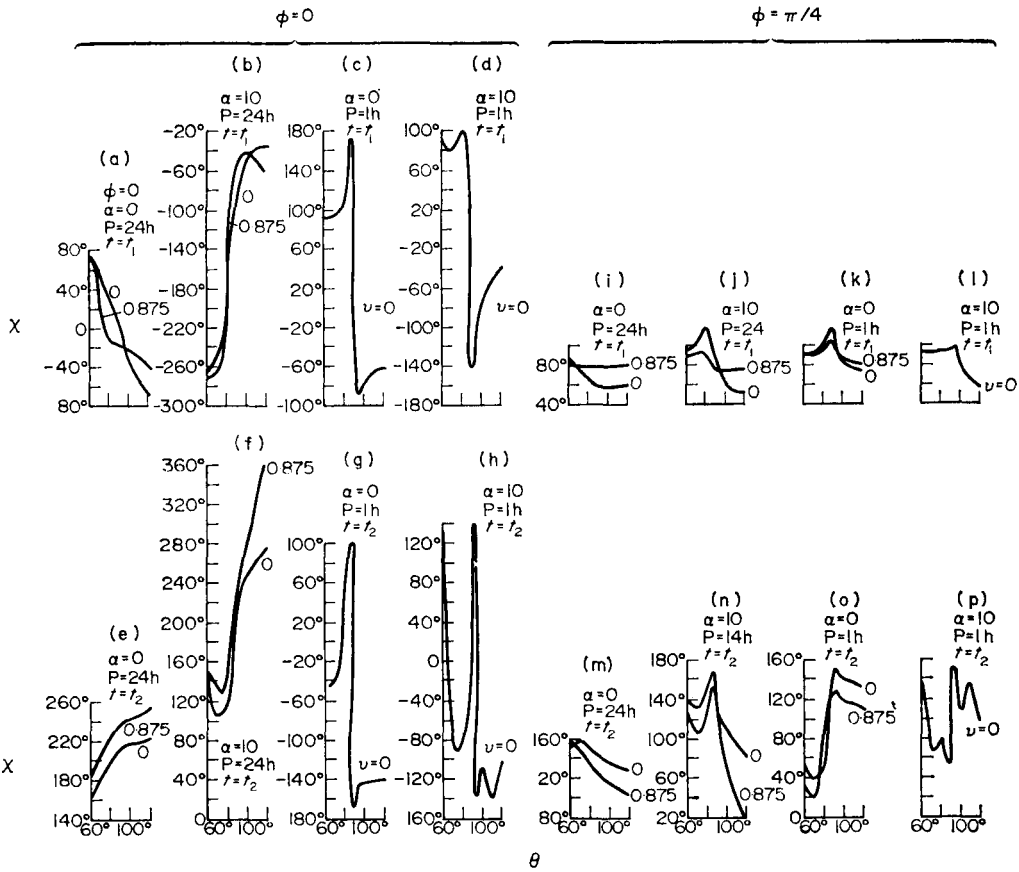

FIG. 14. The angle χ ($= \tan^{-1}(H_\theta^2 + H_\phi^2)^{\frac{1}{2}}/Z$) at which the direction of the total field is inclined to the vertical. The conductors and inducing field are as for Fig. 10. The values of t($t_1 = 0$ and t_2 = a quarter of a period), α(0, or 10), ϕ(0 or $\pi/4$) and the period of variations are indicated on each diagram. The values of ν (0 or 0·875) are indicated on each graph. When the graphs for the two values of ν are almost coincident, only that for $\nu = 0$ is given.

reaches its maximum in sea and is enhanced in both sea and land in the vicinity of the coast. The change in phase for the vertical component near the coastline is gradual and does not amount to a reversal. The amplitude of the horizontal component *normal* to the coastline is enhanced in sea and land provided that the direction of the inducing field is inclined to the axis of the ocean. Otherwise it is enhanced in sea only and falls to the value of the corresponding component of the inducing field at the coastline and in the adjoining land. The change in phase for this component as we cross the coastline is again gradual. The horizontal component parallel to the coastline is only slightly affected.

The direction of the total observed field turns as the coastline is traversed and for short periods this can amount to a reversal in the direction of the total field.

(iii) The enhancement of the components of the total field is more and occurs nearer to the coastline for the shorter periods of variation. For periods of 1 hr or less, the effects are almost the same as for a ' perfectly conducting ' ocean, except that the field is finite at the coastline.

(iv) The coupling between the Earth and the ocean reduces the screening effect of the ocean. For a perfectly conducting Earth at depth *da*, the reduction is about

40–50 per cent if $d = 1/8$ and about 20–30 per cent if $d = 1/5$. Hence, as reported in Paper I, the enhancement in the components of the total field, for periods up to 24 hr, though reduced when both ocean and Earth are taken into account, should be observable within a few hundred kilometres from the coastline for locations at which the continental shelf is itself within a thousand kilometres from the coastline.

(v) Finally, as mentioned before, the modification of the primary field at the coastline and in its vicinity depends on the location of the edge of the continental shelf, the period of variation and the assumed depth of the Earth's conducting core. Hence it is not possible to give a simple table to 'convert' the observed field to the external field in all cases. However the analysis given here and the computer program can be adapted to any particular case by taking suitable values of α, λ and ν, and the required table can then be approximately produced provided there are no further local conductivity anomalies.

Acknowledgments

A major part of the present work was done while the author was a visiting scientist at the National Center for Atmospheric Research*, Boulder, Colorado. Another part was done at the Institut de Physique du Globe, University of Paris, while the writer held a research post from the Centre National de la Recherche Scientifique.

Mathematics Department,
Faculty of Science.
Cairo University,

References

Ashour, A. A., 1964. *Q. J. Mech. appl. Math.*, **17,** 513.
Ashour, A. A., 1965. *Proc. Lond. Math. Soc.*, (3), **15,** 557.
Ashour, A. A., 1971. *Geophys. J. R. astr., Soc.* **22,** 417.
Doss, S. S. & Ashour, A. A., 1971. *Geophys. J. R. astr. Soc.*, **22,** 385.
Kantorovich, L. V. & Krylov, V. I., 1964. *Approximate Methods of Higher Analysis,* translated from Russian by Curtis D. Benster, Interscience, New York.
Smythe, W. R., 1968. *Static and Dynamic Electricity,* Third Edition, McGraw-Hill.

* The National Center for Atmospheric Research is sponsored by the National Science Foundation.